International Journal of Thermophysics, Vol. 1, No. 1, 1980

The Infrared Absorption Coefficient of Alkali Halides

H. H. Li[1]

Received November 5, 1979

Available data on the absorption coefficient of six alkali halides, LiF, NaF, NaCl, KCl, KBr, and KI, were surveyed, evaluated, and analyzed. For the multiphonon absorption region, an equation was formulated to describe the absorption coefficient as a function of both frequency and temperature. Constants in the equation were determined based on data fitting calculations and empirical correlations. The Urbach Rule is applied to the uv absorption edge of the transparent region, and our equation is considered as its counterpart in the IR absorption edge. Comparing with Deutsch's exponential equation, the present expression includes the temperature as an additional independent variable. The calculated values are in concordance with the experimental data.

KEY WORDS: absorption coefficient; optical constants; alkali halides; laser windows.

1. INTRODUCTION

The purpose of this work is to review the available data and information on the absorption coefficient of alkali halides, to critically evaluate, analyze, and to recommend the most probable values of the absorption coefficient. The investigation covers the widest possible wavelength and temperature ranges and is based on data representing the purest samples of alkali halides. However, from the point of view of application, the data analysis is performed only for the IR region.

For a given crystal, the width of the main transparent region is governed by two factors. On the short wavelength side, transmission is restricted by electronic excitation, and for long wavelengths by molecular vibrations and

[1]Center for Information and Numerical Data Analysis and Synthesis, Purdue University, West Lafayette, Indiana 47906, U.S.A.

0195-928X/80/0300-0097$03.00/0

rotations. The width of the transparent spectral range increases as the energy for electronic excitation is increased and that for molecular vibrations decreased. Theoretical and experimental studies on the ionic crystals indicate that crystals having small ions with strong bonding have a wide transparency region; this is true for alkali halides.

Among the various optical properties, those of practical importance are the refractive index and the absorption coefficient. The latter is especially important in the application of high-energy lasers, because many unfavorable effects, which are not observed at low energy levels, are developed at high power levels. No matter how low the absorption is, the effect is objectionable at high-energy levels. As a natural consequence, the magnitude of the absorption coefficient is the key parameter in selecting laser window materials.

Over the past years extensive theoretical and experimental investigations have been conducted in an effort to determine the absorption property for optical materials and to identify the mechanisms influencing the absorption. As a result, numerous measurements and calculations have been reported. However, the available information is discordant and is dispersed throughout the literature.

For this reason, the present work was undertaken. Although all of the alkali halides are, in principle, good optical materials, some of them are intrinsically unsuitable for ordinary applications. They are either physically inadequate or chemically unstable. As a result, available data on the optical constants are concentrated to the following six materials, LiF, NaF, NaCl, KCl, KBr, and KI, which are presented in this work.

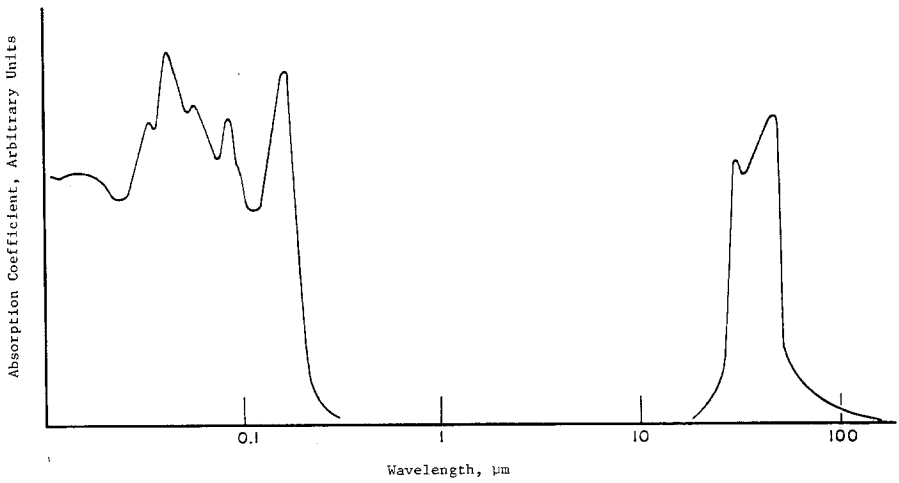

Fig. 1. Typical absorption spectrum of an alkali halide crystal.

2. GENERAL FEATURES OF THE ABSORPTION SPECTRUM OF ALKALI HALIDES

A schematic view of the absorption spectrum of an alkali halide is shown in Fig. 1. At the right (~40 μm) are seen the absorption peaks associated with optical phonons while near the left (~0.15 μm) are the absorption peaks associated with exitons. The spectral positions of these peaks are given in Table I.

The typical behavior of the absorption spectrum is better displayed if one plots the absorption coefficient vs. frequency on a semilogarithmic scale as shown in Fig. 2. Both Figs. 1 and 2 indicate that the fundamental transparent

Table I. Available Parameters for Dispersion Equations of Alkali Halides at Room Temperature

Material	ϵ_0[a]	ϵ_∞[b]	Ultraviolet absorption peaks[c] λ_i (μm)	Infrared absorption peaks[d] λ_I (μm)
LiF	9.04	1.93		32.79, 19.88
LiCl	11.86	2.75	0.130, 0.143	49.26
LiBr	13.23	3.16	0.156, 0.162, 0.173	57.80
LiI	11.03	3.80	0.120, 0.140, 0.167, 0.176, 0.183, 0.197, 0.212	70.42
NaF	5.072	1.174	0.117	40.57
NaCl	5.90	2.33	0.050, 0.100, 0.128, 0.158	60.98, 40.50, 120.34
NaBr	6.396	2.60	0.125, 0.145, 0.176, 0.188	74.63
NaI	7.28	3.01	0.122, 0.141, 0.170, 0.187, 0.228	86.21
KF	5.50	1.85	0.126	51.55
KCl	4.85	2.17	0.131, 0.162	70.42
KBr	4.90	2.36	0.146, 0.173, 0.187	87.72, 60.61
KI	5.09	2.65	0.129, 0.175, 0.187, 0.219	98.04, 69.44
RbF	6.48	1.93	0.115, 0.132	63.29
RbCl	4.92	2.18	0.138, 0.166	85.84
RbBr	4.86	2.34	0.123, 0.146, 0.155, 0.178, 0.191	114.29
RbI	4.94	2.58	0.120, 0.134, 0.156, 0.179, 0.187, 0.223	132.45
CsF	8.08	2.16	0.110, 0.118, 0.136	78.74
CsCl	6.95	2.63	0.119, 0.137, 0.145, 0.162	100.50, 80.00
CsBr	6.38	2.78	0.120, 0.146, 0.160, 0.173, 0.187	136.05, 97.09
CsI	6.31	3.02	0.180, 0.147, 0.163, 0.177, 0.185, 0.206, 0.218	161.29, 117.65

[a]Static dielectric constant data are from Refs. [1–5].

[b]High-frequency dielectric constant data are from Refs. [1,4,6].

[c]The ultraviolet absorption peaks are measured by Hilsch and Pohl [7], Schneider and O'Bryan [8], and Ramachandran [9].

[d]Data sources: see Refs. [1,4]; for LiF, see Ref. [10]; for NaCl, see Ref. [11]; for KBr, see Ref. [12]; for KI, see Ref. [13]; for CsCl, CsBr, and CsI, see Ref. [14].

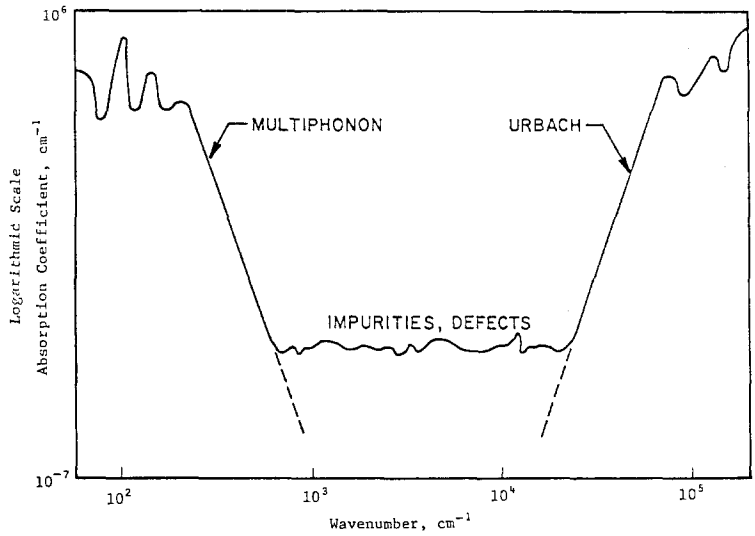

Fig. 2. Schematic absorption spectrum of an alkali halide crystal in semilogarithmic representation.

region of alkali halides is bounded by the Urbach tail and multiphonon absorption. In the high transparent region, the transparency of the material is limited by many factors, notably the crystal vacancies, dislocations, impurities, surface contamination, etc. Extrinsic absorption due to these origins varies considerably depending on the processes of sample preparation and physical environment conditions.

Behavior of the absorption coefficients in the multiphonon and Urbach regions, respectively, suggests an exponential relation between the absorption coefficient and frequency, i.e., $\alpha = \alpha_0 e^{c\nu}$, where α_0 and c are temperature dependent constants. Investigation of the Urbach tail region may serve as an indicator to show the extent of impurity and/or defect contents. As generally observed, the purer the sample, the greater the validity of the Urbach rule is extended into the transparent region. By comparing the absorption spectrum at the Urbach tail, the purer sample is self-revealed. Studies on the Urbach rule have been carried out by many workers, notably Haupt [15], Martienssen [16], Kobayashi and Tomiki [17], Miyata and Tomiki [18], Tomiki and Miyata [19], Sano [20], Tomiki [21], and Tomiki et al. [22]. The result of this work is an expression for the intrinsic absorption coefficient in the tail region, of the form

$$\alpha(E, T) = \alpha_0 \exp\left(\frac{-\sigma_s(T)(E_0 - E)}{kT}\right) \tag{1}$$

where

$$\sigma_s(T) = \sigma_{s0} \frac{2kT}{hf_0} \tanh \frac{hf_0}{2kT}$$

E is the photon energy in units of eV, T is the temperature in units of K, k is the Boltzmann constant, and h is the Planck constant. The parameters α_0, σ_{s0}, E_0, and f_0 for various alkali halides are given in Table II.

Absorption in the multiphonon region has been of current interest because of its application in windows for high-power infrared lasers. At the frequencies in this region, the absorption can be attributed to "intrinsic" processes involving several phonons or to defect modes involving impurities, vacancies, or surface contaminations. Available data in the multiphonon region indicate that the intrinsic absorption coefficient can be expressed as an exponential function of frequency. A number of investigations have been conducted to calculate the frequency and temperature dependence of the intrinsic multiphonon absorption. Deutsch [23] found that the exponential dependence of the absorption coefficient on frequency holds for LiF, NaCl, KCl, and KBr at room temperature, i.e.,

$$\alpha = \alpha_0 e^{-\nu/\nu_0} \tag{2}$$

During the process of data compilation [24] for the present work, we have found that this exponential relation is also applicable in the cases of NaF and KI. The parameters α_0 and ν_0 of various crystals are given in Table III.

In the transparent region, absorption coefficients of a pure crystal are usually low. Crystals with impurities and defects are characterized by the

Table II. The Urbach Parameters of Alkali Halides

Crystal	E_0 (eV)	α_0 (cm^{-1})	hf_0 (meV)	σ_{s0}	Range of E (eV)	Remarks
LiF	13.00	1.0×10^{10}	0.23	0.70	10.6–12.9	Reported by Tomiki and Miyata [19]
NaF	10.70	1.0×10^{10}	16.5	0.69	9.8–10.5	Reported by Tomiki et al. [22]
NaCl	8.025	1.2×10^{10}	9.5	0.741	6.4–7.9	Reported by Tomiki et al. [22]
KCl	7.834	1.26×10^{10}	13.5	0.745	6.4–7.2	Reported by Tomiki et al. [22]
KBr	6.840	6×10^{9}	10.5	0.774	5.3–6.8	Reported by Tomiki et al. [22]
KI	5.890	6×10^{9}	4.5	0.830	4.4–5.8	Reported by Tomiki et al. [22]

Table III. The Parameters of Equation (2)

Crystal	α_0 (cm^{-1})	ν_0 (cm^{-1})	Range of ν (cm^{-1})	Remarks
LiF	2.1317×10^4	153.2	1450–2500	Reported by Deutsch [23]
NaCl	2.4273×10^4	56.0	356–945	Reported by Deutsch [23]
KCl	0.8696×10^4	50.8	317–750	Reported by Deutsch [23]
KBr	0.6077×10^4	39.1	250–600	Reported by Deutsch [23]
NaF	6.1053×10^4	79.5	700–1400	Reported in Ref. [24]
KI	0.4294×10^4	35.1	250–500	Reported in Ref. [24]

appearance of a number of absorption bands, the so-called "color centers." The well-known ones are the *F*, *R*, *M*, and *N* absorption bands. Absorption coefficients at these bands vary considerably with temperature, radiation, and time. Available information on the spectral positions of the color-center peaks is given in Table IV. Color centers can be generated in a crystal by a variety of ways. The most important and common one is by irradiation with ionizing radiation. All the color centers can be bleached either thermally or optically. Both are equivalent in producing annealing.

One of the most important impurities in the crystal is the OH^- radical, whose existence is indicated by the absorption bands located at about 0.2 μm in the ultraviolet and in the range 2.6–2.8 μm in the near infrared. Other stubborn impurities are oxygen containing compounds, which contribute unwanted absorption in the laser wavelength region. Laborious processes of crystal purification do reduce the absorption due to these impurities but seldom eliminate it completely.

Surface absorption appears to be the limiting factor at low absorption levels. The magnitude of surface absorption amounts about 10^{-3} cm^{-2}. At an absorption level of 10^{-6} cm^{-1}, the surface absorption is effectively equivalent to 1000 cm of bulk material! The elimination of surface absorption is therefore an essential phase of sample preparation, the achievement of which is as yet only moderate and uncontrollable.

3. REVIEW OF FUNDAMENTAL ABSORPTION MECHANISMS AND THEORIES

It is convenient to separate the origins that give rise to residual absorption into two classes, the extrinsic and intrinsic. Extrinsic absorptions are those associated with unwanted impurity atoms and molecules, deviations from stoichiometry, lattice defects, and surface contaminations. The intrinsic absorptions are those due to the electronic and vibrational absorptions in an ideal crystal of some specified composition. In practice, extrinsic absorptions

Table IV. Peak Positions (λ_{max}) and Half Widths (W) for the F, R, M, and N Absorption Bands of Alkali Halides[a]

Crystal	Interionic dist., d (Å)	Temp.[b]	F band		R_1 band	R_2 band	M band		N bands
			λ_{max}[c]	W	λ_{max}[c]	λ_{max}[c]	λ_{max}[c]	W	λ_{max}
LiF	2.01	*RT*	(0.254)		(0.295)	(0.320)	(0.416)		
			0.245	0.74	0.306	0.376	0.444		N_1: 0.520
			0.248	0.76	0.308	0.378	0.445		N_2: 0.540
			0.249	0.7	0.310	0.380	0.447		
			0.250		0.313		0.450		
			0.257		0.316				
		NT	0.242	0.47					
		HT	0.243	0.58					
				0.43					
NaF	2.31	*RT*	(0.328)		(0.381)	(0.412)	(0.516)		
			0.335	0.70		0.415	0.505	0.16	
			0.340	0.51			0.507		
			0.341				0.510		
			0.342						
		NT	0.332	0.50			0.498		
		HT	0.336						
NaCl	2.81	*RT*	(0.471)		(0.547)	(0.592)	(0.701)		
			0.458	0.46			0.720		
			0.465	0.47			0.725		
			0.466	0.49					
			0.470	0.50					
		NT	0.448	0.28	0.545	0.596	0.706		0.823
			0.450	0.31			0.713		
			0.452	0.41					
		HT	0.450	0.25					
				0.28					
				0.29					

Table IV. Continued

Crystal	Interionic dist., d (Å)	Temp.[b]	F band		R_1 band	R_2 band	M band		N bands
			λ_{max}[c]	W	λ_{max}[c]	λ_{max}[c]	λ_{max}[c]	W	λ_{max}
KCl	3.14	*RT*	(0.576)		(0.669)	(0.725)	(0.835)		
			0.556	0.31	0.680	0.740	0.820	0.12	
			0.557	0.34			0.822–0.825	0.13	
			0.560	0.35			0.825		
			0.562	0.36			0.830		
			0.563	0.39					
		NT	0.534	0.19	0.650	0.724	0.800–0.820	0.06–0.07	N_1: 0.955
			0.538	0.2	0.656	0.725	0.801–0.802	0.09	N_2: 1.080
			0.539	0.22	0.657	0.727	0.803		N_1: 0.966
			0.540	0.26	0.658	0.729	0.805		$W = 0.08$
			0.543	0.3	0.659	$W = 0.08$	0.808		N_2: 1.028
			0.546		$W = 0.12$				$W = 0.09$
		HT	0.536	0.16			0.798–0.799	0.05–0.06	
			0.537	0.17					
			0.539	0.18					
KBr	3.29	*RT*	(0.630)		(0.732)	(0.792)	(0.897)		
			0.625	0.35			0.917–0.918	0.12–0.13	1.080
			0.628	0.38					
			0.630	0.42					
			0.631						

		NT	0.599	0.19	0.735	0.790	0.887	0.06–0.07
			0.601	0.20			0.892	
			0.603	0.22				
			0.607	0.30				
			0.608					
		HT	0.599	0.16			0.883–0.884	0.05
			0.602	0.20				
KI	3.53	*RT*	(0.718)		(0.834)	(0.902)	(1.000)	
			0.685	0.34				
			0.689	0.35				
			0.692	0.41				
			0.695					
		NT	0.661	0.19				
			0.663	0.21				
			0.664	0.22				
			0.673	0.26				
			0.675					
			0.676					
		HT	0.659	0.14	0.810	0.905	1.010	
			0.666	0.18				
			0.674					
CsI	3.95	*RT*	(0.778)					
			0.785	0.36			1.220	0.1
		NT	0.750	0.23			1.185	0.05

[a]Values were taken from Ref. [25]. λ_{max} is in μm, and W is in eV.
[b]*RT*, reference temperature of 300 K normal; *NT*, liquid nitrogen temperature; *HT*, liquid helium temperature.
[c]Values given in parentheses are calculated from the Ivey relations [26].

appear to be more troublesome in the best of currently available materials, and there are no appropriate means to completely eliminate the objectionable absorptions in optical materials.

In a given crystal, the total absorption can be considered as simply a superposition of the absorptions from various origins. The total absorption coefficient, $\alpha(\nu)$, at frequency ν, is well approximated by

$$\alpha(\nu) = \sum_i N_i \sigma_i(\nu), \tag{3}$$

where the sum is over the various modes and types of imperfection. N_i is the number density of the ith mode or type and σ_i is the corresponding absorption cross-section. In both of the extrinsic and intrinsic absorptions, the processes that give rise to $\sigma_i(\nu)$ may be of three general types: (a) lattice vibration, (b) free-carrier absorption, and (c) electronic excitation.

3.1. Lattice Vibration Absorption

There have been a number of recent studies on how the infrared absorption drops off as the frequency becomes much greater than the fundamental lattice frequencies. These studies have been mainly on the alkali halides and alkaline fluorides. In the highly purified samples, the absorption coefficient exhibits an exponential fall-off over two to four decades to the lowest values of α that can be measured. Whether this exponential absorption tail is characteristic of all other classes of materials is not known.

Presence of impurities can complicate the exponential tail, particularly at low absorption levels. The impurities may enter the lattice singly or multiply in a number of various types of configurations. Unfortunately, the impurity atoms or molecules, which appear to produce troublesome absorptions near 10.6 and 2–5 μm, have not yet been studied adequately. These impurities are primarily the oxygen and hydroxyl radicals whose absorptions are centered at about 3, 9, and 13 μm. The absorption cross-sections due to these impurities are in the range 10^{-18}–10^{-20} cm^2.

3.2. Free-Carrier Absorption

Free carriers, either intrinsic or caused by impurities, contribute a term, α_e, to the absorption that can be correlated roughly with the dc resistivity. Except in the very pure nonpolar crystals, the free-carrier collision time, τ, is on the order of an infrared period (i.e., $\nu\tau \leq 1$). Under this condition, the resistivity at that frequency is not much different from the dc resistivity and can be approximated by the Drude formula

$$\alpha_e(\nu) = \frac{[30/\rho\, n(\nu)]}{(1 + \nu^2\tau^2)}\ \text{cm}^{-1}, \tag{4}$$

where ρ is the dc resistivity in units of ohm cm and $n(\nu)$ is the refractive index at frequency ν. Although free-carrier absorption is negligible for alkali halides, high intensities of the laser beam may increase the free-carrier concentration by photo-excitation.

3.3. Electronic Absorption

In the consideration of infrared transparency of the materials, only those with a bandgap much higher than the infrared frequencies are considered. In the case of alkali halides, electronic excitation contributes little to the infrared absorption. However, the presence of heavy impurities may induce significant IR absorption.

Heavy impurities generally have so low vibration frequencies that the wing of their vibrational absorption contributes negligibly at laser wavelengths. However, heavy impurities may contribute to infrared absorption via their electronic absorption tail. Assuming the impurity electronic absorption is a Lorentzian line at ν_0 and of half width $\Delta\nu$, then the absorption cross-section is given by

$$\sigma_e(\nu) = \tfrac{1}{2} f r_e c \Delta\nu [(\nu - \nu_e)^{-2} - (\nu + \nu_e)^{-2}] \text{ cm}^2 \tag{5}$$

where r_e is the classical electron radius, c is the velocity of light, and $f \sim 1$ is the f number of the transition. In the infrared, where $\nu \ll \nu_e$, Eq. (5) is simplified to

$$\sigma_e(\nu) = 2 f r_e c \frac{\nu \Delta\nu}{\nu_e^3} \tag{6}$$

It is well known that the half width, $\Delta\nu$, of heavy impurities is generally very large and consequently contributes noticeably to absorption in the infrared.

3.4. Surface Absorption

Surface absorption can affect high-power laser window materials in many ways. The heat due to absorption can cause distortions of the optical phase front. In the case of fragile surfaces, such as those of the alkali halides, the surface may develop cracks, which subsequently propagate or enlarge, or become hygroscopic. When antireflection coatings are used, surface absorption may tend to dislodge or evaporate the coatings. The theory of surface absorption may be thought of in terms of the same mechanisms that were discussed for bulk absorption. The most commonly observed surface absorptions are those associated with oxygen and hydroxyl radicals, whose absorptions are centered respectively at 2.8 and 9.3 μm in various crystals.

The fractional power of radiation, α_s, absorbed at the surface, is expressed in the same form as Eq. (3):

$$\alpha_s(\nu) = \sum_i M_i \sigma_i(\nu), \tag{7}$$

where α_s is in units of cm^{-2}, M_i is the number of imperfections of ith type per unit surface area, and σ_i carries the same meaning as in Eq. (3).

3.5. Processes in Multiphonon Absorption

Ever since the advent of high-power infrared lasers, the numerical values of the absorption coefficient of window materials has attracted much attention and has been receiving serious consideration in the wavelength regions where absorption is low. Because the wavelength regions of laser interest are located at the tails of the fundamental absorption bands, a number of theoretical and experimental investigations in the multiphonon absorption region have been carried out in order to define the intrinsic limits on the absorption.

The exponential frequency dependence of the absorption coefficient on the high frequency side of the fundamental absorptance band has been interpreted by a multiphonon absorption theory, in which the fundamental process that contributes to the absorption is that a photon is absorbed by the crystal through the virtual excitation of the fundamental (TO mode) phonon, which in turn emits n phonons. The various processes involved in such a transformation are best demonstrated through a schematic representation. Shown in Fig. 3 are typical processes of n-phonon creation: (a) absorption of a photon and creation of a TO phonon through the dipole moment interaction (open circle), and subsequent decay of the TO phonon into other phonons through anharmonic interactions (closed circles); (b) direct creation of phonons by a photon through higher-order electric moment interactions (open square); (c) the same process as in (b) with subsequent decay of the created phonons; and (d) the sum of all processes of n-phonon creation equivalent to the creation of n phonons by a single process with a "renormalized" nth-order interaction vertex (open hexagon). The anharmonic absorption coefficient, α_A, is the sum of n-phonon absorption, α_n:

$$\alpha_A = \sum_n \alpha_n. \tag{8}$$

3.6. Theories on the Multiphonon Absorption

The bulk of the theories concerning multiphonon absorption were developed during the years 1972–1974. Essential simplification, modification, and improvement of these theories were also made during these years. Currently, our understanding of multiphonon absorption is basically at the same level as in 1974.

The intrinsic absorption may be due to two possible mechanisms: (a) the

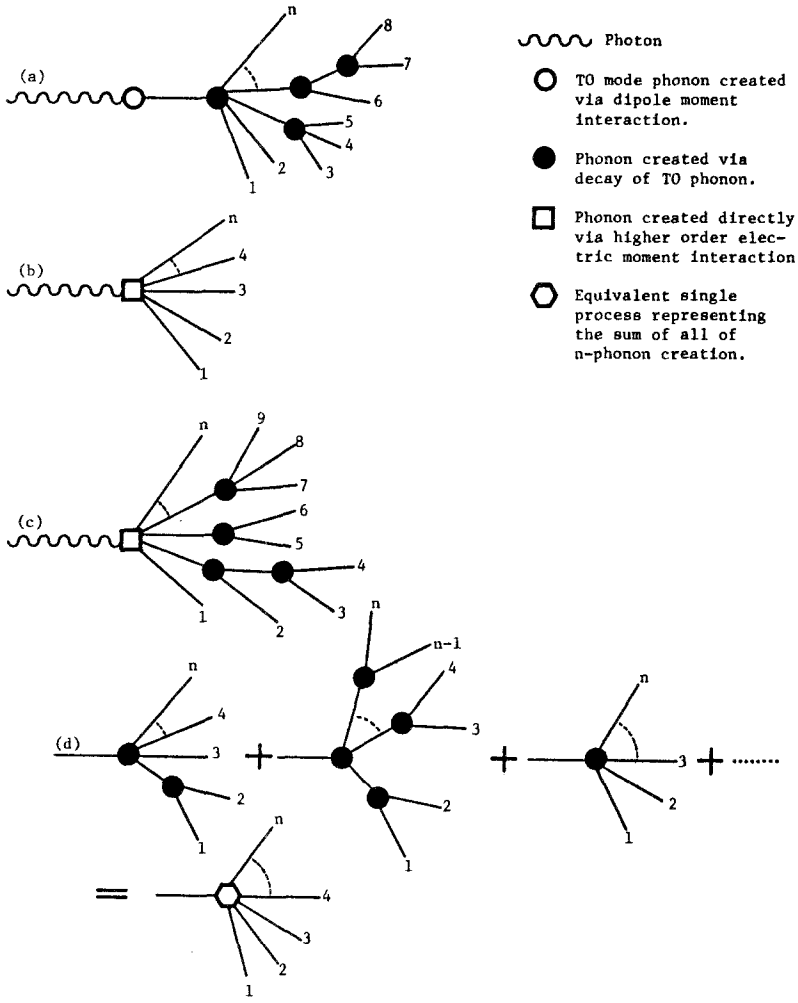

Fig. 3. *n*-Phonon creation processes in multiphonon absorption.

anharmonic coupling of phonons to the fundamental phonon and (b) the displacement-induced electric moment of the ions, which may couple directly to the radiation. The first mechanism is termed as anharmonicity, corresponding to (a) in Fig. 3, and the second as the higher-order moment, corresponding to (b) in Fig. 3. Although these two mechanisms are not totally distinct, as both result physically from charge overlap, traditionally they have been treated differently. For the highly ionic crystals, the constituent molecules are less polarizable, and therefore the effect of the higher-order moment is expected to be less important. As a consequence, the bulk of investigations on ionic crystals has centered on the anharmonically induced absorption.

There are two fundamentally different approaches in the calculation of the anharmonic absorption in ionic crystals. Each of them requires the solution of the harmonic lattice problems followed by a perturbation treatment of the anharmonicity. Sparks and Sham [27, 28] and McGill et al. [29, 30] employed diagrammatic techniques for evaluation of the Green's function, while Bendow et al. [31–35] used the equation-of-motion method. As detailed discussion on the theories is beyond the scope of the present work, the interested reader is referred to additional references [36–43]. Expressions for α_A as obtained in the literature are rather complicated. In the following, we will give the basic part of the expressions from two versions of the theories, that of Sparks and Sham and Bendow et al.

Sparks and Sham [27, 28], in an attempt to explain the nearly exponential behavior of absorption, proposed the n-phonon summation process, in which the photon is absorbed by the crystal through the virtual excitation of the fundamental phonon, which in turn emits n-phonons. In other words, the electromagnetic field drives the fundamental phonon off resonance (since $\nu > \nu_R$), whose relaxation frequency is determined by the sum of all possible processes of splitting the fundamental phonon into n normal modes of lattice vibration. Using the results and notations of Sparks and Sham, the corresponding anharmonic absorption, α_n, as a function of frequency ω, is

$$\alpha_n(\omega) = \frac{4\pi N e^{*2}}{c m_r n_r \Omega} \cdot \frac{\omega \omega_f \Gamma_n(\omega)}{(\omega^2 - \omega_f^2)^2 + [\omega_f \Gamma_n(\omega)]^2} \tag{9}$$

where N is the number of unit cells in a sample of volume Ω, e^* is the Born effective charge, c is the velocity of light, m_r is the reduced mass of the two ions in a unit cell, n_r is the refractive index at ω, ω_f is the frequency of the fundamental mode, and Γ_n is the relaxation frequency of the fundamental mode. It is clear that the central task of the theory is in the calculation of Γ_n. The value of Γ_n can be calculated from the standard peturbation-theory expression for the n-boson-summation relaxation frequency [44]:

$$\Gamma_n(\omega) = \frac{2\pi}{\hbar^2}(n+1)^2 n! \sum_{Q_1 \cdots Q_n} |\Delta(f Q_1 \ldots Q_n)|^2 \Delta(\bar{q}) \delta(\bar{\omega}) \bar{n}_n \tag{10}$$

where Q_j is the phonon mode with wave vector $\bar{q}_j$ and branch b_j, and

$$\bar{q} \text{ is } \sum_{j=1}^{n} \bar{q}_j$$

$$\bar{\omega} \text{ is } \left(\omega - \sum_{j=1}^{n} \omega_{Q_j}\right)$$

Δ is the modified Kronecker δ, which is unity when the argument is zero or a reciprocal-lattice vector and zero otherwise, and

$$\bar{n}_n = \prod_{j=1}^{n} \frac{\bar{n}_j + 1}{\bar{n}_\omega + 1} \tag{11}$$

with

$$\bar{n}_j = n(Q_j) = [\exp(\hbar\omega_{Q_j}/kT) - 1]^{-1} \tag{12}$$

and

$$\bar{n}_\omega = (e^{\hbar\omega/kT} - 1)^{-1} \tag{13}$$

where k is the Boltzman constant and $\bar{n}_j$ and $\bar{n}_\omega$ are Bose-Einstein population factors. The factor, $\Lambda(fQ_1 \ldots Q_n)$ denotes the renormalized vertex corresponding to Fig. 3(d).

Bendow et al. [32] introduced an anharmonic perturbative potential into the Hamiltonian of the phonon. This potential is considered as a portion of the full lattice-interaction potential in the form of a sum of interactions between pairs of atoms in the crystal, under the assumption that the electronic motion is completely separated from the ionic motion (i.e., adiabaticity) and that the point-ion model is valid. As the lattice is set in vibration, the perturbing potential contains cubic or high-order terms of displacement. Their results, when all lengths are scaled in units of the lattice constant a_0, can be written as

$$\alpha_n(\omega) = \frac{\epsilon_0 - \epsilon_\infty}{6\pi c\sqrt{\epsilon_\infty}} \left(\frac{\omega_f}{\omega}\right)^3 \frac{1}{n!} \left(\frac{3}{2}\frac{1}{\mu_D}\right)^{n+1} \left(\frac{\partial^{n+1} V(r)}{\partial \gamma^{n+1}}\right)^2_{r=r_0} \cdot \frac{[\bar{n}(\omega_f) + 1]^2}{\bar{n}(\omega) + 1} M^2 \xi_n, \tag{14}$$

where ϵ_0 is the static dielectric constant, ϵ_∞ is the optical dielectric constant, $\mu_D = \hbar/(\mu\omega_f a_0^2)$ is the dimensionless reduced mass, c is the velocity of light, r_0 is the nearest-neighbor equilibrium spacing, M is the coordination number, ξ_n is the vertex correction factor [28], and $\bar{n}$ is the Bose-Einstein population factor.

Reviewed above are typical theories in the interpretation of multiphonon absorption. Modifications and simplifications have been made by a number of later investigators, notably by Boyer et al. [45] and Harrington et al. [46]. All the theories indicate that corresponding to a given n there is an n-phonon absorption centered at the frequency $n\omega_f$ and that the observed absorption spectrum actually corresponds to the convolution of all possible n's. It is

therefore expected to see structure features in the spectrum. In practice, however, the structure is observable only at low temperatures. At room temperature, the spectrum is well represented by an exponential law of the form of Eq. (2).

3.7. Temperature Dependence of Multiphonon Absorption

Although the existing theories do predict the exponential dependence of the absorption coefficient as a function of frequency at room temperature, with regard to the temperature dependence of absorption, theories have not been very successful. In these theories, the phonons are considered as bosons and thus lead to the following expression:

$$\alpha_n \sim (\bar{n} + 1)^n - (\bar{n})^n \tag{15}$$

where $\bar{n}$ is the usual Bose-Einstein population factor as given in Eqs. (12) and (13). The transition matrix elements are assumed to be essentially temperature independent. After rearrangement of Eq. (15), the coefficient α_A can be expressed as a function of temperature given by

$$\alpha_A \sim \frac{1 - \exp(-n\hbar\bar{\omega}/kT)}{[1 - \exp(-\hbar\bar{\omega}/kT)]^n} \tag{16}$$

where $\bar{\omega}$ is the phonon frequency and $n\bar{\omega} = \omega_{\text{photon}}$.

In the limit where $kT \gg \hbar\bar{\omega}$, we have

$$\alpha_A \sim n\left(\frac{kT}{\hbar\bar{\omega}}\right)^{n-1}$$

or

$$\alpha_A \sim T^{n-1} \tag{17}$$

Disagreement in the value of n is indicated, however, by the best available experimental data [45, 47, 48]. With subsequent modification of the theory by taking into consideration the temperature dependence of the physical parameters used [49], some qualitative improvement is noted.

4. ANALYSIS OF AVAILABLE DATA AND RECOMMENDED VALUES

Absorption in the IR region is of current interest because of its application in windows for high-power infrared lasers. At the frequencies

encountered in this region, the total absorption can be attributed to processes involving several phonons, defect modes due to impurities, vacancies, and surface contaminations. A number of studies have been conducted to investigate the frequency and temperature dependence of the intrinsic multiphonon absorption. It has been found that the exponential dependence of the absorption coefficient on frequency holds for LiF, NaF, NaCl, KCl, KBr, and KI at room temperature.

This exponential relationship attracted considerable attention in the theoretical interpretation of such behavior. Theoretical results indeed predict the exponential dependence of the room temperature absorption coefficient on the frequency. With regard to the temperature dependence, however, the results are not satisfactory. Discrepancies between experimental results and theoretical predictions are of several orders of magnitude. In the case of NaF, NaCl, and KCl, for example, theory predicts that at high temperatures the absorption coefficient varies with temperature according to Eq. (17), where the values of $(n - 1)$ are predicted to be 3, 5, and 6 for NaF, NaCl, and KCl, respectively, while the corresponding experimental values are 2.6, 3.3, and 2.8. As a consequence, many investigators have questioned the validity of the basic assumptions in the transition matrix of Bose-Einstein statistics. It is therefore conceivable that an empirical formula that closely fits the available data should be established until such time when an improved theory becomes available.

4.1. Status of Available Data

Available data on the absorption coefficient of alkali halides were exhaustively compiled from ultraviolet to far infrared regions and were reported in Ref. [24]. Absorption coefficient data, as a whole, are scanty. It is well known that impurities are the major factors that contribute to the total observed absorption. However, the amount of this contribution is generally unknown, partly due to unawareness on the part of investigators and partly due to the inadequacy of the facilities used. As a result, errors are inevitable.

The Urbach rule appears to be generally applicable to the uv absorption edge of alkali halides. Measurements of absorption coefficients as a function of frequency at various temperatures enable the establishment of the equations for the Urbach tails. These equations are useful in predicting the intrinsic absorption coefficients for these materials. Compared with the experimental results at the tails, this rule provides clues regarding the extent of impurity or defect in the samples. To ascertain if the Urbach rule can be extended into the transparent region requires experimental data on ultrapure samples. The current available data are less than adequate to provide such positive evidence.

In the highly transparent region, absorption coefficients are usually low.

Since refractive indices, n, in the transparent region can be measured accurately, the corresponding absorption coefficients can be calculated from the expressions

$$R = \frac{(n-1)^2 + \kappa^2}{(n+1)^2 + \kappa^2} \tag{18}$$

and

$$\alpha = 4\pi\kappa\nu, \tag{19}$$

where κ is the absorption index. It is clear that α can be determined provided that reliable reflectivity data are available. Such important data are currently missing as reflectivity measurements are concentrated in the fundamental uv absorption band and the reststrahlen region.

In the IR region, it has been found that the following facts are common to all of the measurements in the laser wavelength region:

1. Surface absorption predominates at low bulk absorption levels. As a consequence, the observed total absorption is higher than the bulk. The surface absorption band at 9.6 μm is strong enough to mask the intrinsic behavior of the crystal in the wavelength region centered at 9.6 μm.
2. Absorption due to impurities contributes to bulk absorption as well as to surface absorption. At wavelengths of 2.8 and 3.8 μm, absorptions due to hydroxyl ion and oxygen impurities are particularly outstanding.
3. It appears that the above mentioned extrinsic absorptions may render the crystal an unfavorable window material. It has been found, however, that the objectionable extrinsic absorption can be reduced through improved purification and polishing processes.
4. Low total and bulk absorptions, of the order of 10^{-6} cm^{-1} or less, were found at wavelengths of 1.06 and 5.3 μm. Although this value is still very much higher than the respective intrinsic limits, the results represent the limit of instrument sensitivity. Were the sensitivity of the instrument increased considerably, one might be able to observe very low absorption.

Surface contamination is known to contribute to absorption and is usually in the order of 10^{-3} cm^{-1} per unit surface area. At high absorption levels, the effect of surface absorption is negligible. At low absorption levels, say $\alpha < 10^{-3}$ cm^{-1}, surface absorption may predominate over the bulk absorption, resulting in difficulties in the determination of the intrinsic absorption; examples are NaCl and KCl. Additional errors are introduced in

the data available to the end-user, when they must be read off from graphs. The latter errors are unnecessarily contributed in the process of data presentation.

As a result of the combination of above considerations, the errors in data are estimated in general at 3 to 10% in the high absorption range for $\alpha > 0.1$ cm^{-1}. At low absorptions, errors increase with decreased absorption. At very low absorption, errors can be in excess of 100%. As a consequence, intrinsic behavior is only revealed in the high absorption range, while at low levels, the extrinsic factors can predominate and mask the intrinsic.

In special applications, particularly in the area of lasers, high temperature (>300) absorption coefficients are usually needed. It is unfortunate that absorption coefficients are seldom measured at elevated temperatures. The only known systematic measurement of absorption coefficient as a function of frequency and temperature was made by Barker [50] for LiF, NaCl, and KBr. As Barker's values are mostly in the high absorption range and are well behaved, it is highly probably that his results represent the intrinsic absorptions of the corresponding crystals.

4.2. Typical Trends of Data

Typical trends in experimental data (room temperature or higher) can be clearly seen when frequency-dependent absorption coefficients are plotted on a semilog scale (i.e., $\log \alpha$ vs ν) and temperature dependent absorption coefficients are plotted on a log-log scale (i.e., $\log \alpha$ vs $\log T$). Both appear as straight lines in the plots. The implication of this straight line behavior is that the absorption coefficient is related to frequency and temperature, respectively, in the form $\alpha(\nu) \sim e^{-A\nu}$ and $\alpha(T) \sim T^{A'}$, where A and A' are constants for each of the given lines.

The exponential behavior observed in the multiphonon region is similar to the Urbach tail region as shown in Fig. 2. The power law is not only obeyed at the frequencies in the multiphonon region, but the same is also observed in the frequency region on the other side of the fundamental restrahlen band. Readers interested in details of the available data are referred to Ref. [24].

4.3. Formulation of an Empirical Model

A straight line in a semilog plot of $\log \alpha$ vs ν indicates an exponential relation of the form

$$\log \alpha = \log \alpha_0 - 0.43429A(\nu + B) \tag{20}$$

where A is the slope of the line at a given temperature, and α_0 and B are arbitrary constants corresponding to the coordinates of a point on the line.

Therefore three parameters are required to define a straight line in the semilog presentation.

It has been observed that the slopes of these straight lines vary with temperature. This means that α_0 and B also vary with temperature unless there exists a pair of values that is common to all of the lines for a given material. This requirement sets a restriction that all the lines must converge to the point (α_0, B). To see whether this point could be found, a graphical extrapolation was made by drawing straight lines through corresponding data sets and extending them to a region where they tend to meet. Indeed, one does find a definite point of convergence for each of the materials, LiF, NaCl, and KBr. Since adequate data are available at various temperatures, the existence of such a point of convergence provides a reliable clue that α_0 and B are constants for a given material and that only the slope, A, varies with temperature, i.e.,

$$\log \alpha = \log \alpha_0 - 0.43429(\nu + B)A(\mathrm{T}) \tag{21}$$

To find the functional variation of A with T, we have made use of the fact that the plot of α vs T is a straight line on the log-log scale. To meet this condition we are limited to considering the expression

$$A(T) = C(D - \log T), \tag{22}$$

where C and D are constants for a given material. Combining Eqs. (20) and (22) leads to the following empirical equation to represent the absorption coefficient as a function of frequency and temperature:

$$\alpha(\nu, T) = \alpha_0 \exp\left[-a(\nu + b)(c - \log T)\right] \tag{23}$$

where α_0, a, b, and c are constants for a given material. At a given temperature, this equation is reduced to the form $\alpha(\nu) \sim e^{-a'\nu}$, while at a given frequency, the equation is $\alpha(T) \sim T^{b'}$, where a' and b' are constants.

It is interesting to point out that Eq. (23) is analogous to the Urbach rule in the ultraviolet absorption edge. The pair of constants α_0 and b defines the "crossover point," where the curves of α vs ν converge and the factor $a(c - \log T)$ is defined as the "steepness" of the lines. The physical meaning of these parameters remains to be ascertained.

4.4. Numerical Data Fitting for LiF, NaCl, and KBr

Numerical values of the constants α_0, a, b, and c can be defined through least-squares fitting of the experimental data to Eq. (23). Needless to say, the reliability of the values depends on the availability of experimental data and

their accuracies. Review of the existing data indicates that adequate data fitting can be achieved for LiF, NaCl, and KBr. Since the errors in the data are in the range of 10%, the uncertainty in the results of such fitting is at best 10%.

The least-square calculation was performed using the equation

$$\log \alpha = \log \alpha_0 - 0.43429a(\nu + b)(c - \log T) \tag{24}$$

The first approximate values of a and c were evaluated by holding α_0 and b fixed at their graphically determined values. The final values of the constants were then determined by allowing free adjustment of all four constants. The results of the best fit are given in Table V. It was found that, except for LiF, the resulting equation also predicts α values for the molten phase of the materials as if there is no significant change at the phase transition point. This is consistent with Barker's observation.

4.5. Prediction of Key Parameters for NaF, KCl, and KI

Available data for NaF, KCl and KI are not adequate for least-squares calculations in which both frequency and temperature are treated as independent variables. In order to utilize the existing data of these materials and yet give some meaning to the calculations, we have to reduce the number of unknown parameters in Eq. (24). Clues have been observed that enable us to define the parameters a and c for these materials, thus reducing the number of unknown parameters to two.

From careful examination of the list of parameters above, we can see that the values of the parameter c merge as almost a constant for LiF, NaCl, and KBr. The small differences among them can very well be accounted for by errors in the data. Hence it is assumed that an average value of 5.434 may be used as the value of c in Eq. (23) for alkali halides.

Comparing Eq. (23) with Deutsch's representation, Eq. (2), we can see that $1/\nu_0 \sim a(c - \log T)$. At a given temperature, say room temperature, the factor $(c - \log T)$ is a constant, and therefore $1/\nu_0 \sim a$. Indeed, we have found that this is the case for LiF, NaCl, and KBr, for which the values of a

Table V. Values of the Constants α_0, a, b, and c in Eq. (24)

	α_0	a (cm)	b (cm^{-1})	c
LiF	$10^{4.4591}$	0.002237	49.1557	5.39574
NaCl	$10^{5.0505}$	0.005909	83.8511	5.50982
KBr	$10^{4.9073}$	0.008862	93.7115	5.39708

Table VI. Values for Various Parameters of Alkali Halides

	ν_0 (cm^{-1})	a (cm)	$1/a$ (cm^{-1})	M ($g\ mol^{-1}$)	$1/M$ ($mol\ g^{-1}$)	ν_{TO} (cm^{-1})
LiF	153.2	0.002237	447.03	26	0.0385	305
NaF	(78)[a]	(0.00437)	(228.83)	42	0.0238	246.5
NaCl	56.0	0.00591	169.20	58.5	0.0171	164
KCl	50.8	(0.00700)	(142.86)	74.5	0.0134	142
KBr	39.1	0.00886	112.87	120	0.0083	114
KI	(36)	(0.0098)	(102.04)	166	0.0060	102

[a]The values in parentheses are those predicted graphically (see the text).

are obtained from fitting the data. It was noted that the parameter ν_0 is inversely proportional to the molecular weight, M, of the corresponding material [24]. This implies that $1/a$ is related to M in a similar fashion. Listed in Table VI are the values of ν_0, a, $1/a$, M, $1/M$, and ν_{TO} of various materials, where ν_{TO} represents the frequency of the transverse mode fundamental phonon. The inclusion of ν_{TO} here is based on the fact that it was found that ν_{TO} is proportional to ν_0 and $1/a$ as well, except for LiF, as shown in the table.

Figure 4 shows a plot of $1/M$ vs $1/a$ and ν_0. It is seen that the lines of $1/a$ vs $1/M$ and ν_0 vs $1/M$ are parallel to each other, and the points for LiF, NaCl, and KBr on the $1/a$ vs $1/M$ plot precisely define a straight line. Values of a for NaF, Kcl, and KI are thus predicted. Based on the above discussion, one now has only two unknowns in Eq. (23) for NaF, KCl, and KI. What remains is to be done is the evaluation of the parameters α_0 and b.

4.6. Final Results of Data Analysis

Although there is a significant amount of data available for NaF, measured in a wide range of temperatures at a number of discrete frequencies, large uncertainties are inevitably introduced through the rough graphical presentations. As a result, only selected data sets are included in the data fitting calculations.

In the case of KCl, frequency dependence data are only available at room temperature. Although there are temperature-dependent data obtained at 10.6 μm, it is difficult to define the intrinsic bulk absorption because of the extrinsic absorption band at 9.7 μm. As a result, the existing temperature dependence data cannot be used in the determination of α_0 and b, and one has to rely on the room temperature frequency-dependent data to define the values of α_0 and b. In the case of KI, only the room temperature frequency-dependent data are available.

Least-squares data fitting was carried out for NaF, KCl, and KI. For

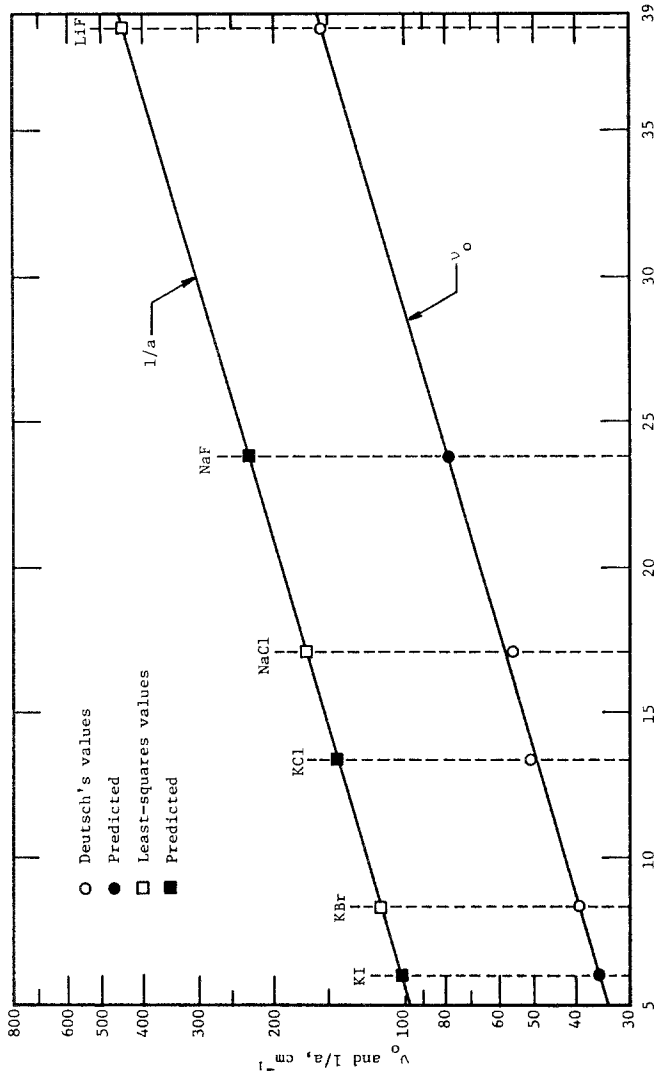

Fig. 4. Plot of ν_0 and $1/a$ of alkali halides as a function of $1/M$.

LiF, NaCl, and KBr, the values of α_0 and b were redefined by least-square fitting. The final results of data fitting yielding the constants α_0, a, b, and c used in Eq. (23) are given in Table VII.

4.7. Recommended and Provisional Values of the Absorption Coefficient

Equation (23) is proposed to yield the absorption coefficient as a function of frequency and temperature in the multiphonon absorption region and in the temperature region where $T \geq 300$ K. Uncertainties in the predicted values are in the range of 10%. In the case of KCl and KI, this uncertainty is applicable to room temperature only. At higher temperatures, a higher uncertainty should be assigned, and the resulting values should be considered as provisional because limited data were available in the determination of the parameters α_0 and b.

Recommended and provisional values are calculated using Eq. (23) and are given in Tables VIII–XIII. For visual demonstration, Figs. 5–10 are provided to show the "crossover point" and the calculated absorption spectra at various temperatures.

5. CONCLUSIONS

In conclusion, it should be emphasized that the present work does not resolve the discrepancies between the available data sets; it simply establishes the most probable values of the absorption coefficient that a pure crystal alkali halide may have with the quoted uncertainties. Also, it should be remembered that, as in any statistical study of this type, Eq. (23) is valid only to the reported accuracy and within the region of experimental data it is based on. In general, extrapolation of the equation for use outside this region is invalid for quantitative results. Finally, the type of analysis presented here assumes the model is an absolutely correct representation of the data at hand, which is not generally true, since the model is an oversimplification of the true behavior of matter. However, for predictive purposes, based on selected

Table VII. Final Values for the Constants α_0, a, b, and c in Eq. (23)

	α_0 (cm^{-1})	a (cm)	b (cm^{-1})	c
LiF	$10^{4.512}$	0.002237	44.1	5.434
NaF	$10^{5.480}$	0.00437	108.4	5.434
NaCl	$10^{4.978}$	0.00591	94.5	5.434
KCl	$10^{6.419}$	0.00700	230.2	5.434
KBr	$10^{4.941}$	0.00886	90.2	5.434
KI	$10^{6.311}$	0.0098	207.3	5.434

Table VIII. Recommended Values on the Infrared Absorption Coefficient of Lithium Fluoride[a]

Wave number (cm^{-1})	Temperature (K)							
	300	300[b]	400	500	600	700	800	1000
1.200E + 03	8.664E + 00	9.9E + 00	1.227E + 01	1.606E + 01	2.002E + 01	2.413E + 01	2.835E + 01	3.713E + 01
1.300E + 03	4.472E + 00	5.6E + 00	6.510E + 00	8.713E + 00	1.105E + 01	1.352E + 01	1.610E + 01	2.154E + 01
1.400E + 03	2.308E + 00	2.5E + 00	3.455E + 00	4.725E + 00	6.103E + 00	7.576E + 00	9.137E + 00	1.250E + 01
1.500E + 03	1.191E + 00	1.3E + 00	1.834E + 00	2.563E + 00	3.369E + 00	4.246E + 00	5.187E + 00	7.250E + 00
1.600E + 03	6.147E − 01	7.0E − 01	9.733E − 01	1.390E + 00	1.860E + 00	2.379E + 00	2.945E + 00	4.206E + 00
1.700E + 03	3.173E − 01	3.4E − 01	5.165E − 01	7.539E − 01	1.027E + 00	1.333E + 00	1.672E + 00	2.440E + 00
1.800E + 03	1.637E − 01	1.7E − 01	2.741E − 01	4.089E − 01	5.668E − 01	7.471E − 01	9.490E − 01	1.415E + 00
1.900E + 03	8.450E − 02	8.2E − 02	1.455E − 01	2.218E − 01	3.129E − 01	4.187E − 01	5.388E − 01	8.212E − 01
2.000E + 03	4.361E − 02	4.2E − 02	7.722E − 02	1.203E − 01	1.727E − 01	2.346E − 01	3.059E − 01	4.764E − 01
2.100E + 03	2.251E − 02	2.1E − 02	4.098E − 02	6.523E − 02	9.537E − 02	1.315E − 01	1.736E − 01	2.764E − 01
2.200E + 03	1.162E − 02	1.1E − 02	2.175E − 02	3.538E − 02	5.265E − 02	7.368E − 02	9.857E − 02	1.603E − 01
2.300E + 03	5.995E − 03	5.9E − 03	1.154E − 02	1.919E − 02	2.906E − 02	4.129E − 02	5.596E − 02	9.302E − 02
2.400E + 03	3.094E − 03		6.126E − 03	1.041E − 02	1.604E − 02	2.314E − 02	3.177E − 02	5.396E − 02

[a]Intrinsic values were calculated according to Eq. (23), with uncertainties about ±10%. Wave number, ν, in cm^{-1}; temperature, T, in K; absorption coefficient, α, in cm^{-1}.

[b]Values in this column, selected from Refs. [23, 47, 51–53], are the total absorption coefficients, which are either the lowest reported or those used to define the constants in Eq. (23). Uncertainties of these values are about ±10%.

Table IX. Recommended Values on the Infrared Absorption Coefficient of Sodium Fluoride[a]

Wave number (cm^{-1})	Temperature (K)							
	300	300[b]	400	500	600	700	800	1000
6.000E + 02	3.198E + 01		4.708E + 01	6.355E + 01	8.120E + 01	9.990E + 01	1.195E + 02	1.614E + 02
6.500E + 02	1.676E + 01		2.536E + 01	3.496E + 01	4.545E + 01	5.674E + 01	6.877E + 01	9.481E + 01
7.000E + 02	8.784E + 00	7.4E + 00	1.366E + 01	1.923E + 01	2.544E + 01	3.223E + 01	3.956E + 01	5.570E + 01
7.500E + 02	4.604E + 00		7.356E + 00	1.058E + 01	1.424E + 01	1.831E + 01	2.275E + 01	3.273E + 01
8.000E + 02	2.413E + 00	2.7E + 00	3.962E + 00	5.821E + 00	7.971E + 00	1.040E + 01	1.309E + 01	1.923E + 01
8.500E + 02	1.265E + 00		2.134E + 00	3.202E + 00	4.461E + 00	5.905E + 00	7.529E + 00	1.130E + 01
9.000E + 02	6.627E − 01	8.0E − 01	1.149E + 00	1.762E + 00	2.497E + 00	3.354E + 00	4.331E + 00	6.638E + 00
9.434E + 02	3.783E − 01	5.5E − 01	6.717E − 01	1.049E + 00	1.509E + 00	2.053E + 00	2.680E + 00	4.183E + 00
9.500E + 02	3.473E − 01		6.190E − 01	9.691E − 01	1.398E + 00	1.905E + 00	2.491E + 00	3.900E + 00
1.000E + 03	1.820E − 01		3.334E − 01	5.331E − 01	7.823E − 01	1.082E + 00	1.433E + 00	2.291E + 00
1.050E + 03	9.541E − 02		1.796E − 01	2.933E − 01	4.379E − 01	6.145E − 01	8.242E − 01	1.346E + 00
1.100E + 03	5.000E − 02	4.6E − 02	9.672E − 02	1.613E − 01	2.451E − 01	3.490E − 01	4.741E − 01	7.909E − 01
1.150E + 03	2.621E − 02		5.209E − 02	8.876E − 02	1.372E − 01	1.983E − 01	2.727E − 01	4.647E − 01
1.200E + 03	1.373E − 02		2.806E − 02	4.883E − 02	7.679E − 02	1.126E − 01	1.569E − 01	2.730E − 01
1.250E + 03	7.198E − 03		1.511E − 02	2.686E − 02	4.298E − 02	6.396E − 02	9.024E − 02	1.604E − 01
1.300E + 03	3.773E − 03	4.8E − 03	8.139E − 03	1.478E − 02	2.406E − 02	3.633E − 02	5.191E − 02	9.424E − 02
1.350E + 03	1.977E − 03		4.384E − 03	8.130E − 03	1.347E − 02	2.063E − 02	2.986E − 02	5.537E − 02
1.400E + 03	1.036E − 03	1.4E − 03	2.361E − 03	4.472E − 03	7.537E − 03	1.172E − 02	1.717E − 02	3.253E − 02

[a]Intrinsic values were calculated according to Eq. (23), with uncertainties about ±10%. Wave number, ν, in cm^{-1}; temperature, T, in K; absorption coefficient, α, in cm^{-1}.

[b]Values in this column, selected from Refs. [48, 51, 52, 54–56], are the total absorption coefficients, which are either the lowest reported or those used to define the constants in Eq. (23). Uncertainties of these values are about ±10%.

Table X. Recommended Values on the Infrared Absorption Coefficient of Sodium Chloride[a]

Wave number (cm^{-1})	Temperature (K)							
	300	300[b]	400	500	600	700	800	1000
4.000E + 02	1.679E + 01		2.419E + 01	3.211E + 01	4.047E + 01	4.921E + 01	5.830E + 01	7.739E + 01
4.500E + 02	7.008E + 00		1.048E + 01	1.431E + 01	1.846E + 01	2.290E + 01	2.760E + 01	3.770E + 01
5.000E + 02	2.925E + 00	2.5E + 00	4.537E + 00	6.377E + 00	8.422E + 00	1.066E + 01	1.306E + 01	1.836E + 01
5.500E + 02	1.221E + 00	1.2E + 00	1.965E + 00	2.842E + 00	3.842E + 00	4.958E + 00	6.184E + 00	8.945E + 00
6.000E + 02	5.095E − 01	5.7E − 01	8.509E − 01	1.267E + 00	1.753E + 00	2.307E + 00	2.927E + 00	4.357E + 00
6.500E + 02	2.127E − 01	2.7E − 01	3.685E − 01	5.644E − 01	7.997E − 01	1.074E + 00	1.386E + 00	2.122E + 00
7.000E + 02	8.876E − 02	1.0E − 01	1.596E − 01	2.515E − 01	3.648E − 01	4.996E − 01	6.559E − 01	1.034E + 00
7.500E + 02	3.705E − 02	4.1E − 02	6.911E − 02	1.121E − 01	1.664E − 01	2.325E − 01	3.105E − 01	5.036E − 01
8.000E + 02	1.546E − 02	1.4E − 02	2.993E − 02	4.996E − 02	7.593E − 02	1.082E − 01	1.470E − 01	2.453E − 01
8.500E + 02	6.454E − 03	4.6E − 03	1.296E − 02	2.227E − 02	3.464E − 02	5.033E − 02	6.957E − 02	1.195E − 01
9.000E + 02	2.694E − 03		5.614E − 03	9.923E − 03	1.580E − 02	2.342E − 02	3.293E − 02	5.821E − 02
9.434E + 02	1.262E − 03	1.0E − 03	2.715E − 03	4.920E − 03	7.996E − 03	1.206E − 02	1.721E − 02	3.118E − 02
9.500E + 02	1.124E − 03		2.431E − 03	4.422E − 03	7.209E − 03	1.090E − 02	1.559E − 02	2.836E − 02
1.000E + 03	4.693E − 04		1.053E − 03	1.971E − 03	3.289E − 03	5.071E − 03	7.380E − 03	1.381E − 02
1.050E + 03	1.959E − 04		4.560E − 04	8.783E − 04	1.500E − 03	2.360E − 03	3.493E − 03	6.728E − 03
1.100E + 03	8.175E − 05		1.975E − 04	3.914E − 04	6.845E − 04	1.098E − 03	1.654E − 03	3.278E − 03
1.887E + 03	8.703E − 11	3.4E − 05	3.759E − 10	1.169E − 09	2.956E − 09	6.473E − 09	1.277E − 08	3.971E − 08
2.632E + 03		5.3E − 05						
3.700E + 03								
9.434E + 03		7.0E − 06						

[a]Intrinsic values were calculated according to Eq. (23), with uncertainties about ±10%. Wave number, ν, in cm^{-1}; temperature, T, in K; absorption coefficient, α, in cm^{-1}.

[b]Values in this column, selected from Refs. [23, 46–48, 57, 58], are the total absorption coefficients, which are either the lowest reported or those used to define the constants in Eq. (23). Uncertainties of these values are about ±10%. Values lower than 1.0E − 03 carry higher uncertainties up to ±30%.

Table XI. Recommended Values on the Infrared Absorption Coefficient of Potassium Chloride[a]

Wave number (cm^{-1})	Temperature (K)							
	300	300[b]	400	500	600	700	800	1000
4.000E + 02	5.667E + 00		9.835E + 00	1.508E + 01	2.139E + 01	2.873E + 01	3.711E + 01	5.691E + 01
4.500E + 02	2.013E + 00	1.1E + 00	3.650E + 00	5.790E + 00	8.442E + 00	1.161E + 01	1.530E + 01	2.428E + 01
5.000E + 02	7.153E − 01	4.6E − 01	1.355E + 00	2.223E + 00	3.332E + 00	4.692E + 00	6.311E + 00	1.036E + 01
5.500E + 02	2.541E − 01	1.6E − 01	5.028E − 01	8.536E − 01	1.315E + 00	1.896E + 00	2.603E + 00	4.418E + 00
6.000E + 02	9.027E − 02	6.2E − 02	1.866E − 01	3.277E − 01	5.192E − 01	7.662E − 01	1.073E + 00	1.885E + 00
6.500E + 02	3.207E − 02	2.4E − 02	6.925E − 02	1.258E − 01	2.050E − 01	3.096E − 01	4.426E − 01	8.041E − 01
7.000E + 02	1.139E − 02	8.8E − 03	2.570E − 02	4.831E − 02	8.090E − 02	1.251E − 01	1.825E − 01	3.430E − 01
7.500E + 02	4.048E − 03	3.2E − 03	9.539E − 03	1.855E − 02	3.193E − 02	5.055E − 02	7.526E − 02	1.463E − 01
8.000E + 02	1.438E − 03	1.3E − 03	3.540E − 03	7.121E − 03	1.261E − 02	2.043E − 02	3.104E − 02	6.243E − 02
8.500E + 02	5.108E − 04	1.0E − 04	1.314E − 03	2.734E − 03	4.976E − 03	8.255E − 03	1.280E − 02	2.663E − 02
9.000E + 02	1.815E − 04	1.0E − 04	4.877E − 04	1.050E − 03	1.964E − 03	3.336E − 03	5.278E − 03	1.136E − 02
9.434E + 02	7.391E − 05	1.2E − 04	2.063E − 04	4.573E − 04	8.765E − 04	1.519E − 03	2.446E − 03	5.424E − 03
9.500E + 02	6.447E − 05		1.810E − 04	4.031E − 04	7.753E − 04	1.348E − 03	2.176E − 03	4.847E − 03
1.000E + 03	2.290E − 05	6.5E − 03	6.717E − 05	1.548E − 04	3.060E − 04	5.447E − 04	8.975E − 04	2.068E − 03
1.050E + 03	8.137E − 06	9.0E − 05	2.493E − 05	5.942E − 05	1.208E − 04	2.201E − 04	3.701E − 04	8.821E − 04
1.100E + 03	2.891E − 06		9.253E − 06	2.281E − 05	4.768E − 05	8.894E − 05	1.526E − 04	3.763E − 04
1.150E + 03	1.027E − 06		3.434E − 06	8.759E − 06	1.882E − 05	3.594E − 05	6.294E − 05	1.605E − 04
1.200E + 03	3.648E − 07	4.8E − 04	1.274E − 06	3.363E − 06	7.430E − 06	1.452E − 05	2.596E − 05	6.848E − 05
1.250E + 03	1.296E − 07	6.0E − 05	4.730E − 07	1.291E − 06	2.933E − 06	5.869E − 06	1.070E − 05	2.922E − 05
1.300E + 03	4.605E − 08		1.756E − 07	4.957E − 07	1.158E − 06	2.372E − 06	4.414E − 06	1.246E − 05
1.887E + 03		4.2E − 06						
2.632E + 03		5.6E − 05						
3.700E + 03		5.9E − 05						

[a]Intrinsic values were calculated according to Eq. (23), with uncertainties about ±10%. Wave number, ν, in cm^{-1}; temperature, T, in K; absorption coefficient, α, in cm^{-1}. Values at temperatures other than 300 K are provisional values.

[b]Values in this column, selected from Refs. [23, 45, 47, 48, 58–65], are the total absorption coefficients, which are either the lowest reported or those used to define the constants in Eq. (23). Uncertainties of these values are about ±10%. Values lower than 1.0E − 03 carry higher uncertainties up to ±30%.

Table XII. Recommended Values on the Infrared Absorption Coefficient of Potassium Bromide[a]

Wave number (cm^{-1})	Temperature (K)							
	300	300[b]	400	500	600	700	800	1000
3.000E + 02	3.171E + 00	2.0E + 00	4.885E + 00	6.829E + 00	8.980E + 00	1.132E + 01	1.383E + 01	1.934E + 01
3.250E + 02	1.647E + 00		2.609E + 00	3.726E + 00	4.986E + 00	6.379E + 00	7.896E + 00	1.128E + 01
3.500E + 02	8.558E − 01	7.0E − 01	1.393E + 00	2.033E + 00	2.769E + 00	3.595E + 00	4.508E + 00	6.578E + 00
3.750E + 02	4.446E − 01		7.440E − 01	1.109E + 00	1.538E + 00	2.026E + 00	2.573E + 00	3.837E + 00
4.000E + 02	2.309E − 01	2.0E − 01	3.973E − 01	6.053E − 01	8.538E − 01	1.142E + 00	1.469E + 00	2.238E + 00
4.250E + 02	1.200E − 01		2.122E − 01	3.303E − 01	4.741E − 01	6.436E − 01	8.386E − 01	1.305E + 00
4.500E + 02	6.232E − 02	1.8E − 02	1.133E − 01	1.802E − 01	2.633E − 01	3.627E − 01	4.787E − 01	7.613E − 01
4.750E + 02	3.237E − 02		6.052E − 02	9.833E − 02	1.462E − 01	2.044E − 01	2.733E − 01	4.440E − 01
5.000E + 02	1.682E − 02	1.3E − 02	3.232E − 02	5.365E − 02	8.117E − 02	1.152E − 01	1.560E − 01	2.590E − 01
5.250E + 02	8.735E − 03		1.726E − 02	2.927E − 02	4.507E − 02	6.493E − 02	8.907E − 02	1.511E − 01
5.500E + 02	4.538E − 03	4.0E − 03	9.218E − 03	1.597E − 02	2.503E − 02	3.659E − 02	5.084E − 02	8.810E − 02
5.750E + 02	2.357E − 03		4.923E − 03	8.715E − 03	1.390E − 02	2.062E − 02	2.903E − 02	5.139E − 02
6.000E + 02	1.225E − 03	1.5E − 03	2.629E − 03	4.755E − 03	7.718E − 03	1.162E − 02	1.657E − 02	2.997E − 02
9.433E + 02	1.521E − 07	1.4E − 05	4.774E − 07	1.160E − 06	2.394E − 06	4.420E − 06	7.517E − 06	1.826E − 05
1.887E + 03		5.6E − 05						
2.632E + 03		1.7E − 04						
3.700E + 03		1.2E − 04						
9.434E + 03		3.0E − 06						

[a]Intrinsic values were calculated according to Eq. (23), with uncertainties about ±10%. Wave number, ν, in cm^{-1}; temperature, T, in K; absorption coefficient, α, in cm^{-1}.

[b]Values in this column, selected from Refs. [23, 46, 47, 57, 65, 66], are the total absorption coefficients, which are either the lowest reported or those used to define the constants in Eq. (23). Uncertainties of these values are about ±10%. Values lower than 1.0E − 03 carry higher uncertainties up to ±30%.

Table XIII. Recommended Values on the Infrared Absorption Coefficient of Potassium Iodide[a]

Wave number (cm^{-1})	Temperature (K)							
	300	300[b]	400	500	600	700	800	1000
2.500E + 02	3.598E + 00	2.7E + 00	6.298E + 00	9.724E + 00	1.387E + 01	1.872E + 01	2.427E + 01	3.747E + 01
2.750E + 02	1.744E + 00		3.147E + 00	4.975E + 00	7.233E + 00	9.925E + 00	1.305E + 01	2.064E + 01
3.000E + 02	8.450E − 01	7.8E − 01	1.572E + 00	2.546E + 00	3.774E + 00	5.264E + 00	7.022E + 00	1.137E + 01
3.250E + 02	4.095E − 01	4.9E − 01	7.857E − 01	1.303E + 00	1.969E + 00	2.791E + 00	3.777E + 00	6.262E + 00
3.500E + 02	1.984E − 01	2.2E − 01	3.926E − 01	6.665E − 01	1.027E + 00	1.480E + 00	2.032E + 00	3.449E + 00
3.750E + 02	9.616E − 02	1.2E − 01	1.962E − 01	3.410E − 01	5.358E − 01	7.850E − 01	1.093E + 00	1.900E + 00
4.000E + 02	4.660E − 02	4.3E − 02	9.801E − 02	1.745E − 01	2.795E − 01	4.163E − 01	5.879E − 01	1.047E + 00
4.250E + 02	2.258E − 02	2.2E − 02	4.897E − 02	8.928E − 02	1.458E − 01	2.208E − 01	3.162E − 01	5.765E − 01
4.500E + 02	1.094E − 02	1.0E − 02	2.447E − 02	4.568E − 02	7.607E − 02	1.171E − 01	1.701E − 01	3.175E − 01
4.750E + 02	5.303E − 03	6.7E − 03	1.223E − 02	2.337E − 02	3.969E − 02	6.209E − 02	9.150E − 02	1.749E − 01
5.000E + 02	2.570E − 03	4.5E − 03	6.109E − 03	1.196E − 02	2.070E − 02	3.293E − 02	4.922E − 02	9.635E − 02

[a]Intrinsic values were calculated according to Eq. (23), with uncertainties about ±10%. Wave number, ν, in cm^{-1}; temperature, T, in K; absorption coefficient, α, in cm^{-1}.

[b]Values in this column, selected from Refs. [46, 67, 68], are the total absorption coefficients, which are either the lowest reported or those used to define the constants in Eq. (23). Uncertainties of these values are about ±10%.

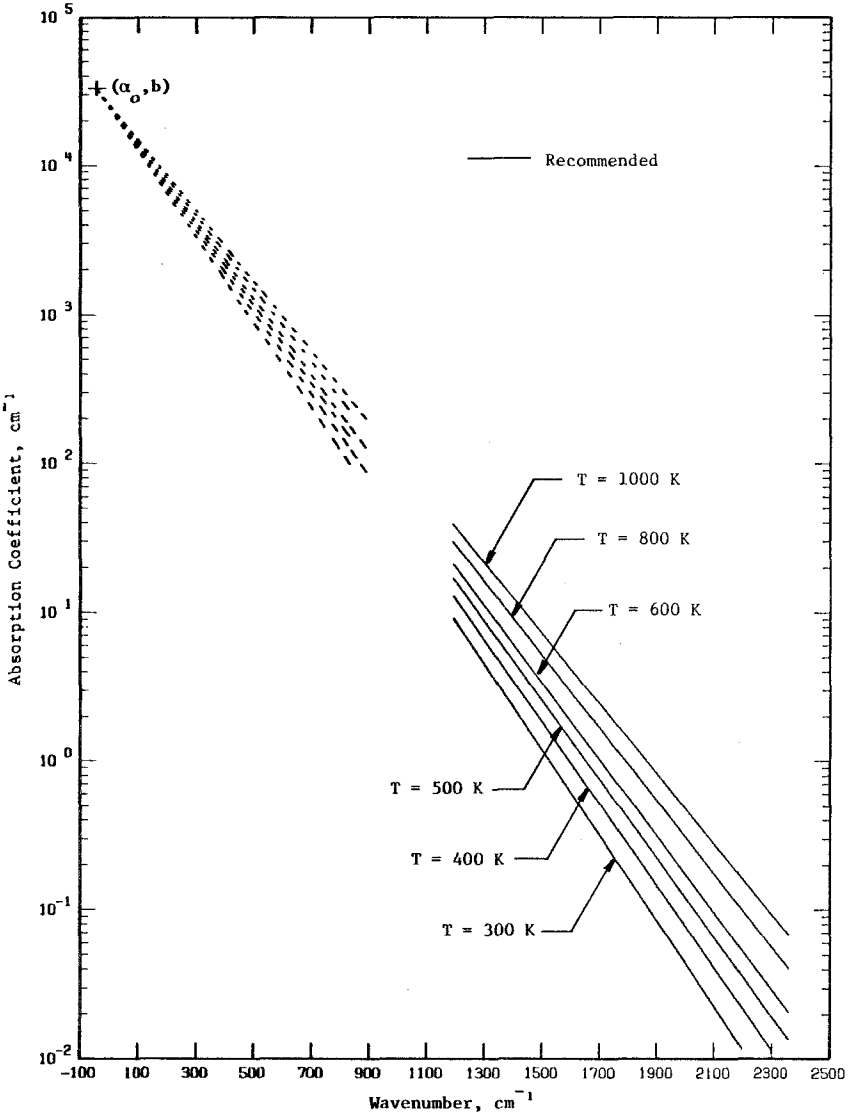

Fig. 5. Recommended absorption spectra of lithium fluoride.

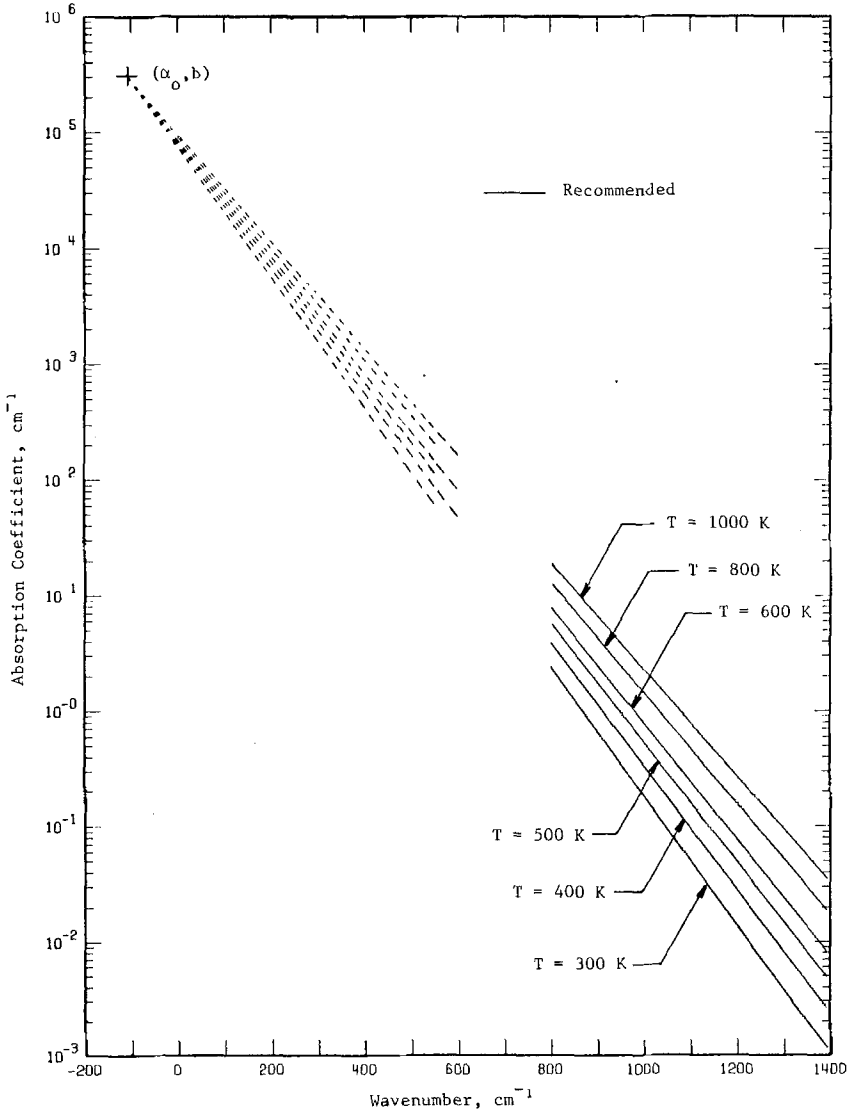

Fig. 6. Recommended absorption spectra of sodium fluoride.

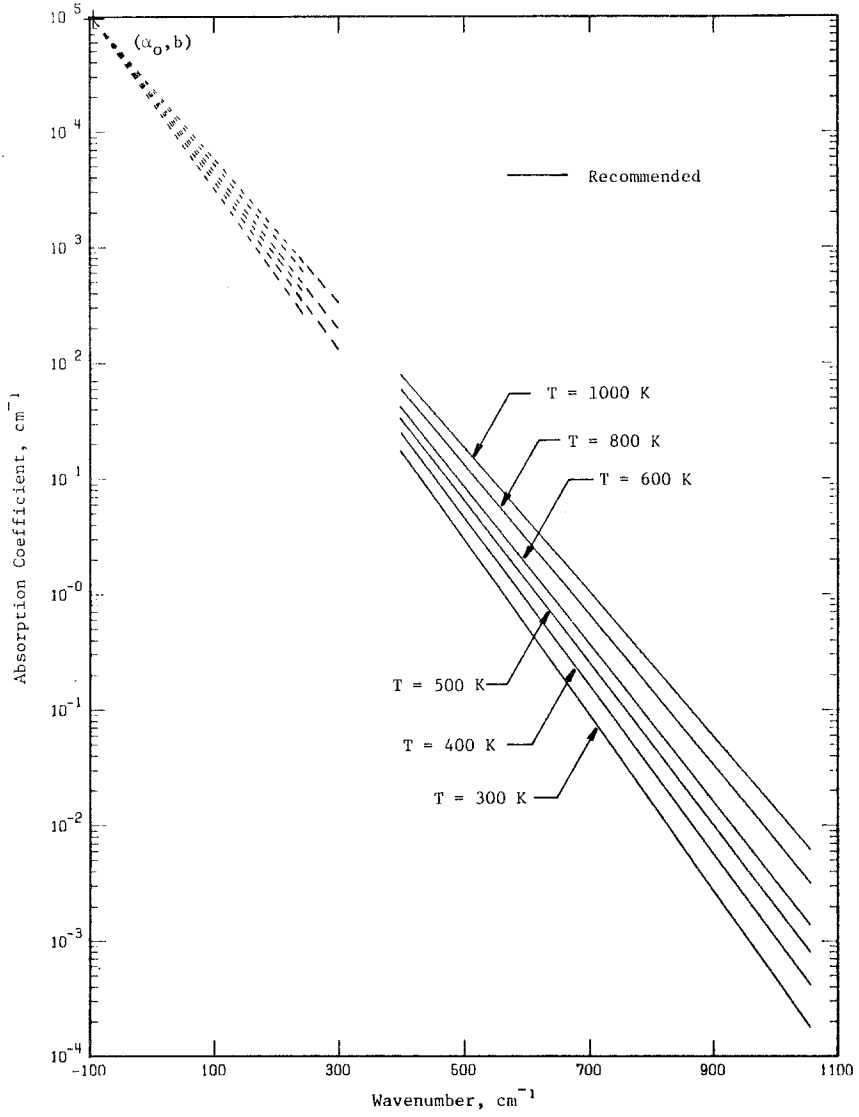

Fig. 7. Recommended absorption spectra of sodium chloride.

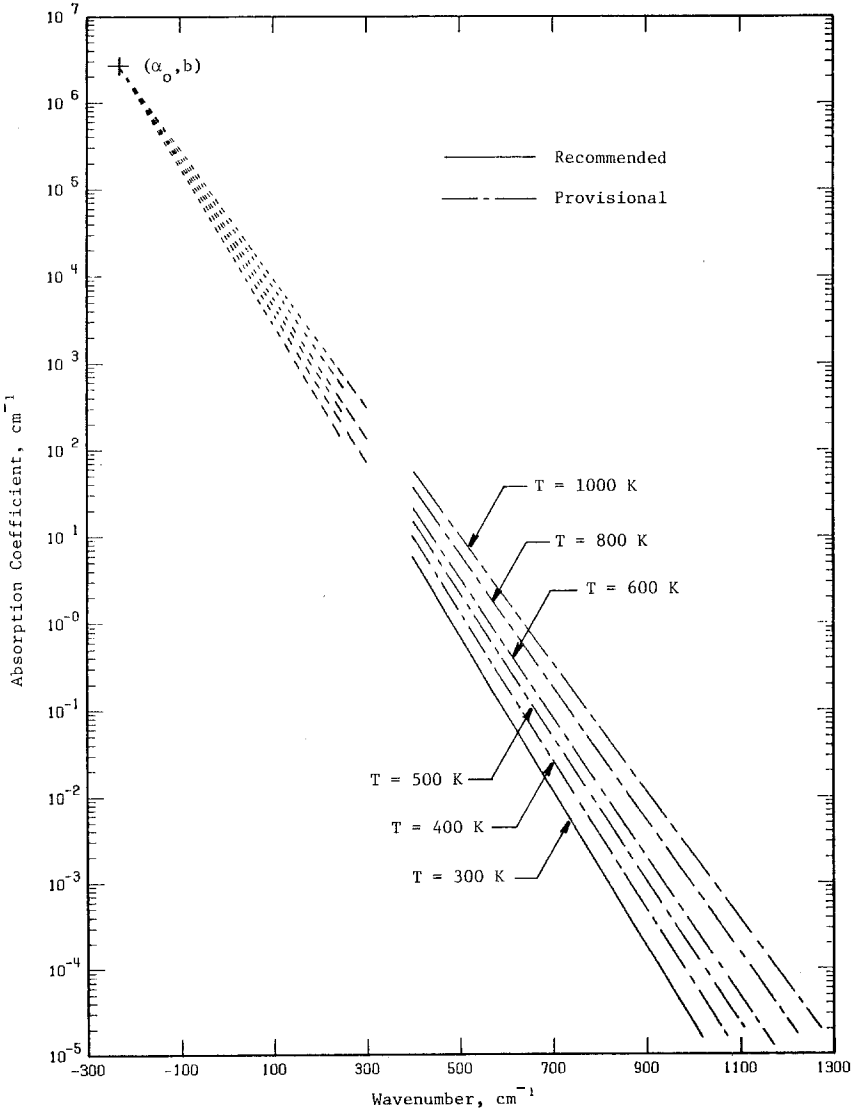

Fig. 8. Recommended absorption spectra of potassium chloride.

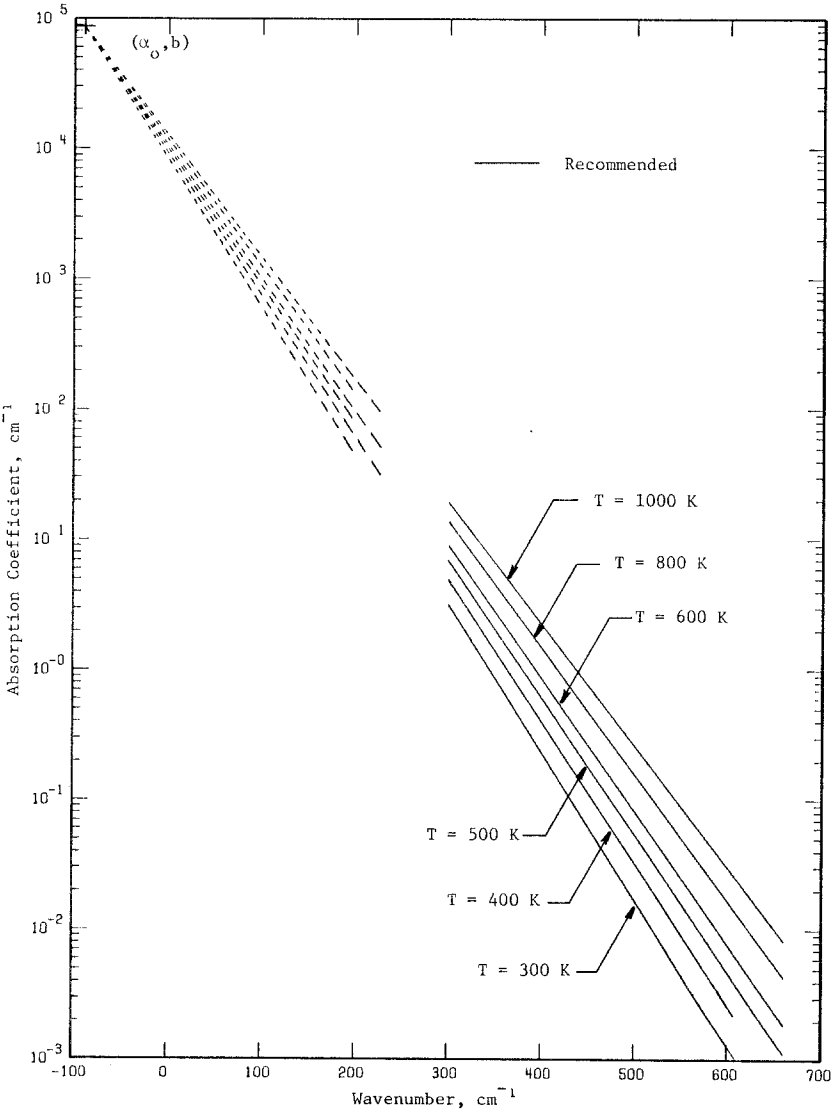

Fig. 9. Recommended absorption spectra of potassium bromide.

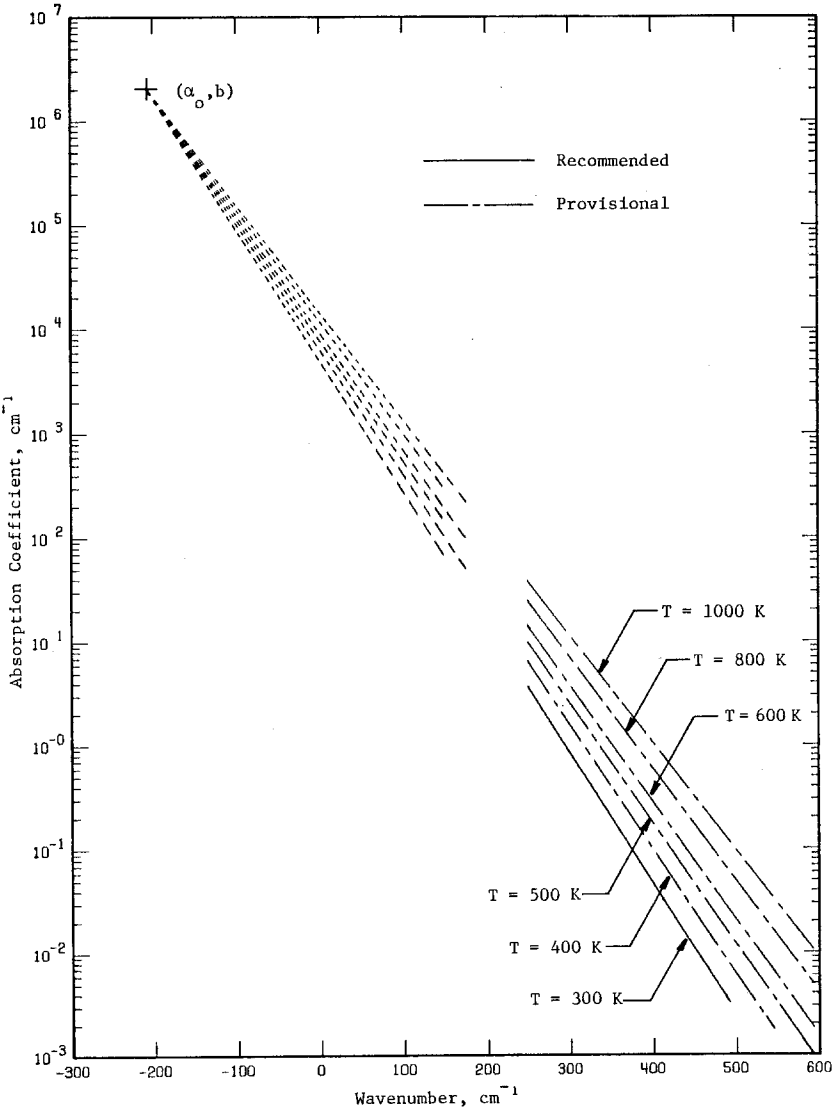

Fig. 10. Recommended absorption spectra of potassium iodide.

experimental data from several sources, and within the usable region of the data, we believe that Eq. (23) is valid for calculation of the absorption coefficient in the given wavelength and temperature regions. It is important to point out that the relationship established in the present work is restricted to the temperature region where $T \geq 300$ K.

ACKNOWLEDGMENT

This work was supported by the Air Force Office of Scientific Research (AFSC), United States Air Force.

REFERENCES

1. R. P. Lowndes and D. H. Martin, *Proc. Rog. Soc. London* **A308:** 473 (1969).
2. R. P. Lowndes, *Phys. Lett.* **21**(1): 26 (1966).
3. C. Andeen, J. Fontanella, and S. Donald, *Phys. Rev.* **B2**(12): 5068 (1970).
4. E. Kartheuser, *Polarons in Ionic Crystals and Polar Semiconductors*, J. T. Devreese, ed. North-Holland/American Elsevier, 1972, p. 717.
5. K. F. Young and H. P. R. Frederikse, *J. Phys. Chem. Ref. Data* **2**(2): 313 (1973).
6. J. W. Hodby, J. A. Borders, and F. C. Brown, *Phys. Rev. Lett.* **19**(17): 952 (1967).
7. R. Hilsch and R. W. Pohl, *Z. Phys.* **59**: 812 (1930).
8. E. G. Schneider and H. M. O'Bryan, *Phys. Rev.* **51**(5): 293 (1937).
9. G. N. Ramachandran, *Proc. Indian Acad. Sci.* **25A:** 481 (1947).
10. J. R. Jasperse, A. Kahan, and J. N. Plendl, *Phys. Rev.* **146**(2): 526 (1966).
11. L. Genzel, H. Happ, and R. Weber, *Z. Phys.* **154:** 13 (1959).
12. A. Handi, J. Çlaudel, D. Chanal, P. Strimer, and P. Vergnat, *Phys. Rev.* **163**(3): 836 (1967).
13. A. Handi, J. Claudel, G. Morlot, and P. Strimer, *Appl. Opt.* **7**(1): 161 (1968).
14. P. Vergnat, J. Claudel, A. Handi, P. Strimer, and F. Vermillard, *J. Phys.* **30**(8–9): 723 (1969).
15. U. Haupt, *Z. Phys.* **157:** 232 (1959).
16. W. Martienssen, *J. Phys. Chem. Solids* **2:** 257 (1957).
17. K. Kobayashi and T. Tomiki, *J. Phys. Soc. Jpn.* **16**(7): 1417 (1961).
18. T. Miyata and T. Tomiki, *J. Phys. Soc. Jpn.* **22**(1): 209 (1967).
19. T. Tomiki and T. Miyata, *J. Phys. Soc. Jpn.* **27**(3): 658 (1969).
20. R. Sano, *J. Phys. Soc. Jpn.* **27**(3): 695 (1969).
21. T. Tomiki, *J. Phys. Soc. Jpn.* **21:** 403 (1966).
22. T. Tomiki, T. Miyata, and H. Tsukamoto, *Z. Naturforsch.* **29A:** 145 (1974).
23. T. F. Deutsch, *J. Phys. Chem. Solids* **34:** 2091 (1973).
24. H. H. Li, CINDAS Rept. 54 (1979).
25. W. D. Compton and H. Rabin, *Solid State Phys.* **16:** 121 (1964).
26. H. F. Ivey, *Phys. Rev.* **72:** 341 (1947).
27. M. Sparks and L. J. Sham, *Solid State Commun.* **11:** 1451 (1972).
28. M. Sparks and L. J. Sham, *Phys. Rev. B* **8**(6): 3037 (1973).
29. T. C. McGill, R. W. Hellworth, and M. Mangir, *J. Phys. Chem. Solids* **34:** 2105 (1973).
30. T. C. McGill and H. V. Winston, *Solid State Commun.* **13:** 1459 (1973).
31. B. Bendow and S. C. Ying, *Phys. Lett. A* **42**(5): 359 (1973).
32. B. Bendow, S.C. Ying, and S. P. Yukon, *Phys. Rev. B* **8**(4): 1679 (1973).
33. B. Bendow, *J. Electron. Mater.* **3**(1): 101 (1974).
34. B. Bendow and P. D. Gianino, *Opt. Commun.* **9**(3): 306 (1973).
35. B. Bendow, S. P. Yukon, and S. C. Ying., *Phys. Rev.* **10**(6): 2286 (1974).
36. D. L. Mills and A. A. Maradudin, *Phys. Rev. B* **8**(4): 1617 (1973).

37. D. L. Mills and A. A. Maradudin, *Phys. Rev. B* **10**(4): 1713 (1974).
38. K. V. Namjoshi and S. S. Mitra, *Phys. Rev. B* **9**(2): 815 (1974).
39. H. B. Rosenstock, *Phys. Rev. B* **9**(4): 1963 (1974).
40. C. J. Duthler and M. Sparks, *Laser Induced Damage in Optical Materials*, Proc. 6th ASTM-ONR-NBS Symp. (National Bureau of Standards, Washington, DC, 1974), p. 219.
41. A. A. Maradudin and D. L. Mills, *Phys. Rev. Lett.* **31**(11): 718 (1973).
42. B. Bendow, *Appl. Phys. Lett.* **23**(3): 133 (1973).
43. J. R. Hardy and B. S. Agrawal, *Appl. Phys. Lett.* **22**(5): 236 (1973).
44. M. Sparks, *Ferromagnetic-Relaxation Theory* (McGraw-Hill, New York, 1964).
45. L. L. Boyer, J. A. Harrington, M. Hass, and H. B. Rosenstock, *Phys. Rev. B* **11**(4): 1665 (1975).
46. J. A. Harrington, C. J. Duthler, F. W. Patten, and M. Hass, *Solid State Commun.* **18:** 1043 (1976).
47. J. M. Rowe and J. A. Harrington, *Phys. Rev. B* **14**(12): 5442 (1976).
48. J. A. Harrington and M. Hass, *Phys. Rev. Lett.* **31**(11): 710 (1973).
49. T. C. McGill and H. V. Winston, *Solid State Commun.* **13:** 1459 (1973).
50. A. J. Barker, *J. Phys. C* **5** 2276 (1972).
51. H. W. Hohls, *Ann. Phys.* **29:** 433 (1937).
52. M. Klier, *Z. Phys.* **150:** 49 (1958).
53. A. Kachare, M. P. Soriaga, and G. Andermann, *J. Opt. Soc. Am.* **64**(11): 1450 (1974).
54. H. Beck and D. W. Pohl, *Proceedings of the Second International Conference on Phonon Scattering Solids* (Plenum, New York, 1976), p. 361.
55. T. F. McNelly and D. W. Pohl, *Phys. Rev. Lett.* **32**(23): 1305 (1974).
56. D. W. Pohl and P. F. Meier, *Phys. Rev. Lett.* **32**(2): 58–61 (1974).
57. S. Califano and M. Czerny, *Z. Phys.* **150:** 1 (1958).
58. S. D. Allen and J. A. Harrington, *Appl. Opt.* **17**(11): 1679 (1978).
59. M. Hass, J. W. Davison, P. H. Klein, and L. L. Boyer, *J. Appl. Phys.* **45**(9): 3959 (1974).
60. T. F. Deutsch, *Appl. Phys. Lett.* **25**(2): 109 (1974).
61. E. F. Shrader, U.S. Air Force Rept. AFML-TR-74-165 (1974), p. 79.
62. M. Hass, J. W. Davison, H. B. Rosenstock, and J. Babiskin, *Appl. Opt.* **14**(5): 1128 (1975).
63. H. B. Rosenstock, D. A. Gregory, and J. A. Harrington, *Appl. Opt.* **15**(9): 2075 (1976).
64. J. M. Rowe and J. A. Harrington, *J. Appl. Phys.* **47**(11): 4926 (1976).
65. A. Mentzel, *Z. Phys.* **88:** 178 (1934).
66. P. H. Klein, J. W. Davison, and J. A. Harrington, *Mater. Res. Bull.* **11:** 1335 (1976).
67. J. I. Berg and E. E. Bell, *Phys. Rev. B* **4**(10): 3572 (1971).
68. J. E. Eldridge and K. A. Kembry, *Phys. Rev. B* **8**(2): 746 (1973).